Int. J. Solids Structures, Vol. 11, pp. 233–246. Pergamon Press 1975. Printed in Great Britain

ON THE SEPARATION OF GEOMETRIC AND VISCOELASTIC DISPERSION IN COMPOSITE MATERIALS†

HERBERT J. SUTHERLAND
Shock Wave Phenomena Division 5163, Sandia Laboratories,
Albuquerque, New Mexico 87115, U.S.A.

(*Received* 14 *December* 1973)

Abstract—With the completion of an experimental study of the dispersion characteristics of fiber-reinforced viscoelastic materials, a sufficient body of information has been generated to demonstrate the feasibility of separating viscoelastic dispersion from the total dispersion spectrum of this class of material. The basic procedure for the separation is to construct a homogeneous viscoelastic constitutive equation for the composite and to use cross plots of the viscoelastic characterization with the total dispersion spectrum of the composite to reveal the influence of viscoelastic dispersion on the total spectrum. Two methods of constructing the homogeneous model are discussed and the results are compared with experimental data.

INTRODUCTION

The dispersion characteristics of a composite material with a viscoelastic constituent is determined by two dispersive mechanisms. The first, viscoelastic dispersion, results from the viscoelastic nature of the composite, and the second, geometric dispersion, results from the internal geometry of the composite. Either of these two mechanisms may dominate the other or they may act in unison, depending on the time scale of the experiment and the particular composite used. To help clarify the roles played by these two mechanisms, two methods have been devised to separate viscoelastic dispersion from the total dispersion spectrum of a viscoelastic composite. The methods are detailed in this paper and two examples are offered.

Recently, Sutherland[1] has completed a study of the dispersive characteristics of two fiber-reinforced viscoelastic materials. The first composite studied was a cloth-laminate quartz phenolic (2D-QP). Its dispersion characteristics (both phase velocity and attenuation vs frequency) were obtained at seven temperatures, ranging from 4·4 to 40·0°C. The second material studied was stainless steel wires embedded in an Epon 828-Z matrix (EPON-SST). Its dispersion characteristics (phase velocity vs frequency) were determined at five temperatures, ranging from 5·0 to 41·7°C.

With this information, the separation of viscoelastic dispersion from the total dispersion spectrum of this class of composites may be demonstrated. The basic procedure for the separation is to construct a homogeneous viscoelastic constitutive equation for the composite and to use cross plots of the viscoelastic characterization with the total dispersion spectrum of the composite to reveal the influence of viscoelastic dispersion on the total spectrum.

This paper details two methods by which the homogeneous viscoelastic characterization may be obtained for a particular composite, and the methods are illustrated using the data cited above. The first method used to construct the homogeneous characterization employs the low-frequency dispersion spectrum of the composite at several temperatures and the principle of time–temperature superposition. This method is not dependent on a knowledge of the constituent

†This work was supported by the United States Atomic Energy Commission.

properties and is illustrated using the 2D-QP data. The second method employs a quasi-static homogeneous model that has been proposed to describe the behavior of unidirectional wires in a viscoelastic matrix. When the model is transformed to the dynamic regime, it allows one to predict the dynamic, homogeneous viscoelastic behavior of the composite from the constituent's properties. This method is illustrated using the EPON-SST data.

ANALYSIS

Viscoelastic analysis

In one dimension, let us assume that for low strain rates the composite behaves as a linear, homogeneous viscoelastic solid; namely, its response to small displacement gradients $\partial u(X, t)/\partial X$ (i.e. small strains at the material point X and time t) is governed by the linear hereditary law [2, 3]

$$\sigma(X, t) = G(0)\frac{\partial u(X, t)}{\partial X} + \int_0^\infty G'(s)\frac{\partial u(X, t-s)}{\partial X}\,\mathrm{d}s \tag{1}$$

for σ the longitudinal stress. The function $G(s)$ is the longitudinal stress relaxation function and $G'(s) = \mathrm{d}G(s)/\mathrm{d}s$. Here we are interested in solutions of Eq. (1) and the dynamical field equation for a traveling sinusoidal wave. The solution has the form†

$$u(X, t) = u_0 \operatorname{Re}\{\exp[-(\alpha + i\omega/C)X]\exp(i\omega t)\}. \tag{2}$$

In general for viscoelastic materials, the phase velocity $C>0$ and the attenuation $\alpha > 0$ will be functions of the frequency $\omega > 0$. In fact, it has been shown [4] that the solution (2) is admissible if and only if

$$\rho_R C^2(\omega) = |G(0) + \bar{G}'(\omega)|\sec^2[\tfrac{1}{2}\nu(\omega)], \tag{3}$$

$$\alpha(\omega) = [\omega/C(\omega)]\tan[\tfrac{1}{2}\nu(\omega)], \tag{4}$$

where ρ_R is the reference density, the phase angle $\nu(\omega)$, $0 \le \nu < \frac{1}{2}\pi$, is defined by

$$\tan\nu(\omega) = \frac{\operatorname{Im}[G(0) + \bar{G}'(\omega)]}{\operatorname{Re}[G(0) + \bar{G}'(\omega)]}, \tag{5}$$

and $\bar{G}'(\omega)$ is the Fourier transform

$$\bar{G}'(\omega) = \int_0^\infty G'(s)\exp(-i\omega s)\,\mathrm{d}s. \tag{6}$$

Assuming that the temperature dependence of G may be incorporated into Eq. (1) through a time shift that is defined by the principle of time–temperature superposition,‡ the effect of a temperature change from T_1 to T_0 is to shift the time scale by a factor of a_t.§ Thus, if $G(t)$ is

†The notation Re and Im are used to denote the real and imaginary parts of a complex function.

‡The assumption that the principle of time–temperature superposition holds for the composite is based on the fact that if this principle holds for the viscoelastic matrix, then the homogeneous model of Hashin [5] indicates that it holds for the composite. See also Sutherland and Calvit [6] for further verification of this assumption.

§The longitudinal stress relaxation modulus $G(t)$ also will be shifted by the temperature change from T_1 to T_0, see Ferry [7]. This shift is small in comparison to experimental errors and is not considered in this analysis.

known at temperature T_0 then at T_1, $G(t)$ is given by

$$G(t)|_{T=T_1} = G(t/a_t)|_{T=T_0}. \tag{7}$$

Ferry[7] has shown that a_t is related to a temperature change in the following manner:

$$\log_{10}(a_t) = -\frac{\Delta H_a}{R}\left(\frac{1}{T_1} - \frac{1}{T_0}\right), \quad T_1 < T_g, \tag{8}$$

where ΔH_a is the apparent activation energy for the relaxation or retardation processes, R is the gas constant, T_g is the glass transition temperature, and T_0 is the reference temperature. Introducing the time–temperature shift factor into Eq. (1),

$$\sigma(X, t/a_t) = G(0)\frac{\partial u(X, t/a_t)}{\partial X} + \int_0^\infty G'(s/a_t)\frac{\partial u\left(X, \dfrac{t-s}{a_t}\right)}{\partial X}\mathrm{d}s. \tag{9}$$

Sutherland and Calvit[6] have shown that the solution of Eq. (9) proceeds as described above, and that the effect of a temperature change on the phase velocity C and attenuation α is

$$C(\omega)|_{T=T_1} = C(\omega a_t)]_{T=T_0}, \tag{10}$$

$$\alpha(\omega)|_{T=T_1} = a_t\alpha(\omega a_t)|_{T=T_0}. \tag{11}$$

Equations (10) and (11) describe the superposition of frequency (time) and temperature. Thus, if the phase velocity and attenuation are known as a function of temperature at some frequency (or a function of frequency at some temperature), the phase velocity and attenuation are known for all temperatures and frequencies, within the limits of applicability of Eq. (8).

For the composite, Eqs. (10) and (11) imply that if the phase velocity and attenuation are known in a frequency range where geometric dispersion is small, then data in this range, taken at various temperatures, can be used to determine the high-frequency viscoelastic response of the homogeneous counterpart to the composite. Thus, the composite's viscoelastic constitutive equation can be obtained over a wide frequency range, without the inclusion of geometric dispersion, and cross plots of this viscoelastic characterization with actual composite dispersion spectra will reveal the contribution of viscoelastic dispersion to the total dispersion spectrum.

Homogeneous characterization

Another method by which the homogeneous viscoelastic constitutive equation may be obtained for the composite is to use one of the homogeneous constitutive models that have been proposed to predict the quasi-static response of this class of materials. Here, we are concerned with unidirectional elastic fibers embedded in a viscoealstic matrix. Hashin[5] has proposed a model which obtains specific relations or upper and lower bounds for the independent moduli in this transversely isotropic material. Following his example, one may determine that the lower bound for the longitudinal stress relaxation modulus, G, perpendicular to unidirectional rigid fibers is given by

$$G(t) = G_m(t)\left\{1 + \frac{v_f}{v_m}\left[1 + \frac{2(1-2\mu_m(t))}{3-4\mu_m(t)}\right]\right\}, \tag{12}$$

where G_m is longitudinal stress relaxation modulus for the matrix material, v_f is the volume fraction of fibers, v_m is the volume fraction of the matrix, and μ_m is Poisson's ratio for the matrix.

As the matrix is usually relatively weak compared to embedded fibers, this lower bound for rigid fibers is probably a very good approximation for the actual quasi-static response of the composite.

Using Eq. (12) and the viscoelastic analysis discussed previously (Eqs. (1) through (6)), the homogeneous dynamic response of the composite may be determined. If we assume that Poisson's ratio for the matrix is not a function of time, then the velocity of an acoustic wave in the composite, without the effects of internal geometry, is given in terms of velocity function of the matrix $C_m(\omega)$ by

$$C(\omega) = C_m(\omega)\sqrt{\frac{\rho_m}{\rho}}\sqrt{1+\frac{v_f}{v_m}\left[1+\frac{2(1-2\mu_m)}{3-4\mu_m}\right]}, \tag{13}$$

where ρ_m is the density of the matrix, and ρ is the density of the composite.

EXPERIMENTAL PROGRAM

Composite materials

The dispersion spectra for two fiber-reinforced viscoelastic materials have been obtained by Sutherland[1]. The first composite studied was a cloth-laminate quartz phenolic (2D-QP). Typical cross sections are shown in Fig. 1. The phase velocity and attenuation dispersion spectra, for harmonic waves traveling perpendicular to the fibers, were obtained at seven temperatures (40·0°C, 34·4°C, 27·8°C, 22·2°C, 15·6°C, 10·0°C, and 4·4°C). Least squares curve fits of the data are plotted in Figs. 2, 3 and 4 and summarized in Tables 1 and 2. The second composite studied was

Table 1. Velocity dispersion spectra for quartz phenolic $C = A_0 + A_1 x + A_2 x^2$ (mm/μsec)

Independent variable (x)	Temperature T (°C)	Frequency ω (MHz)	A_0	A_1	A_2
T	$-5 \le T \le 45$	1·0	3·655	−0·3392 E−2	—
ω	40·0	$0{\cdot}5 \le \omega \le 2{\cdot}6$	3·499	0·3749 E−1	−0·1711 E−1
ω	34·4	$0{\cdot}5 \le \omega \le 2{\cdot}8$	3·534	0·1314 E−1	−0·8203 E−2
ω	27·8	$0{\cdot}5 \le \omega \le 3{\cdot}0$	3·550	0·2266 E−1	−0·1176 E−1
ω	22·2	$0{\cdot}5 \le \omega \le 4{\cdot}0$	3·578	0·5685 E−2	−0·3562 E−2
ω	15·6	$0{\cdot}5 \le \omega \le 4{\cdot}0$	3·605	0·1035 E−2	−0·2716 E−2
ω	10·0	$0{\cdot}5 \le \omega \le 4{\cdot}3$	3·610	0·1618 E−1	−0·5334 E−2
ω	4·4	$0{\cdot}5 \le \omega \le 4{\cdot}4$	3·628	0·1738 E−1	−0·5227 E−2

Table 2. Attenuation dispersion spectra for quartz phenolic $C = A_0 + A_1\omega + A_2\omega^2$ (nepers/mm)

Temperature T (°C)	Frequency ω (MHz)	A_0	A_1	A_2
40·0	$1{\cdot}4 \le \omega \le 2{\cdot}6$	0·9444 E−1	−0·8964 E−1	0·3486 E−1
34·4	$1{\cdot}4 \le \omega \le 2{\cdot}7$	0·3673 E−1	−0·3328 E−1	0·2057 E−1
27·8	$1{\cdot}4 \le \omega \le 2{\cdot}8$	0·8955 E−1	−0·8152 E−1	0·3053 E−1
22·2	$1{\cdot}4 \le \omega \le 3{\cdot}2$	0·1103	−0·1015	0·3409 E−1
15·6	$1{\cdot}4 \le \omega \le 3{\cdot}3$	0·6304 E−1	−0·5636 E−1	0·2347 E−1
10·0	$1{\cdot}4 \le \omega \le 3{\cdot}6$	0·4318 E−1	−0·3946 E−1	0·2005 E−1
4·4	$1{\cdot}4 \le \omega \le 3{\cdot}6$	0·6456 E−1	−0·5867 E−1	0·2400 E−1

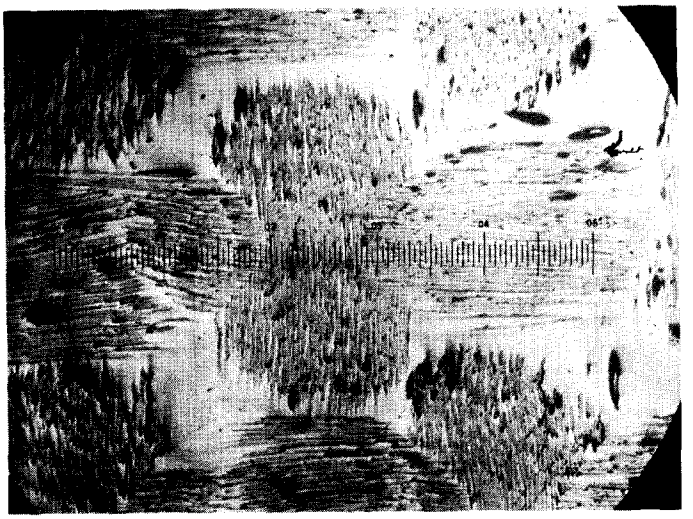

50 X

Fig. 1(a)

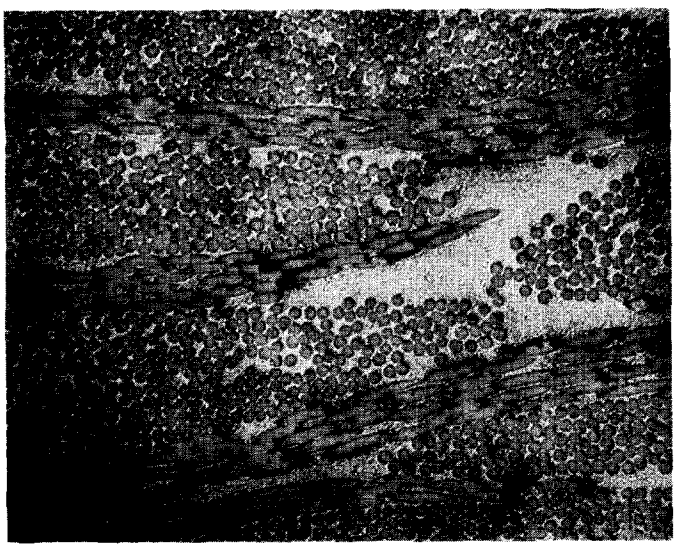

100 X

Fig. 1(b)

Fig. 1. Typical cross sections of quartz phenolic.

stainless steel wires embedded in an Epon 828-Z matrix. A typical cross section is shown in Fig. 5. The phase velocity dispersion spectra, for harmonic waves traveling perpendicular to the fibers, were obtained at five temperatures (41·7°C, 31·7°C, 22·2°C, 13·3°C and 5·0°C). Least squares curve fits of the data are plotted in Fig. 6 and summarized in Table 3.

A complete description of the material properties and fabrication techniques for these two composite materials is contained in the Appendix.

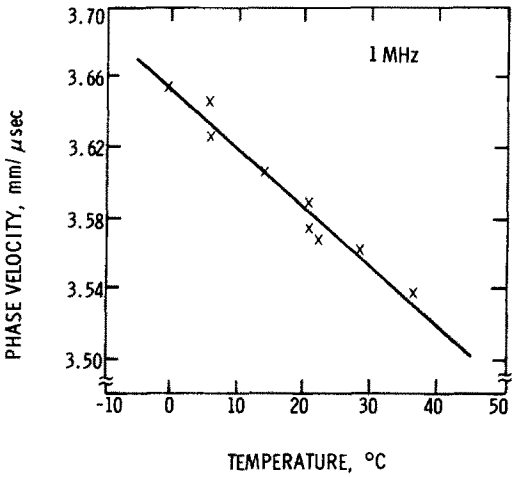

Fig. 2. Temperature data for quartz phenolic.

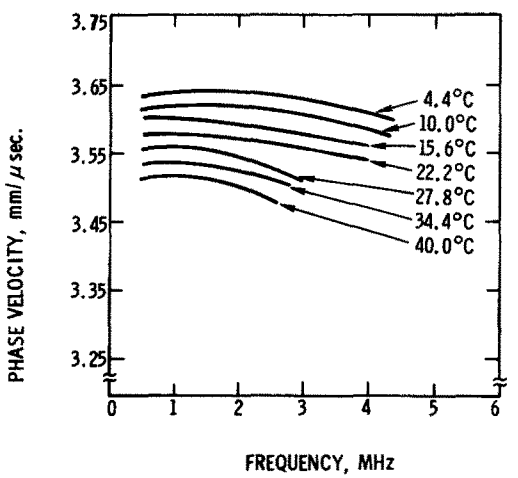

Fig. 3. Velocity dispersion spectra for quartz phenolic at various temperatures.

Table 3. Velocity dispersion spectrum for EPON-SST $C = A_0 + A_1x + A_2x^2$ (mm/μsec)

Independent variable (x)	Temperature T (°C)	Frequency ω (MHz)	A_0	A_1	A_2
T	$-10 \le T \le 65$	0·5	2·047	−0·3577 E−2	—
ω	41·7	$0{\cdot}4 \le \omega \le 0{\cdot}9$	1·865	0·3876	−0·6444
ω	31·7	$0{\cdot}4 \le \omega \le 0{\cdot}9$	1·846	0·5370	−0·7232
ω	22·2	$0{\cdot}4 \le \omega \le 0{\cdot}9$	1·983	0·2229	−0·5057
ω	13·3	$0{\cdot}4 \le \omega \le 0{\cdot}8$	2·012	0·1593	−0·3722
ω	5·0	$0{\cdot}4 \le \omega \le 0{\cdot}8$	1·920	0·5950	−0·7532

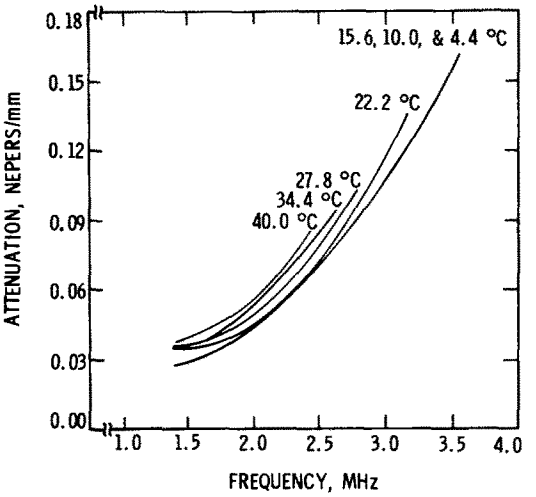

Fig. 4. Attenuation dispersion spectra for quartz phenolic at various temperatures.

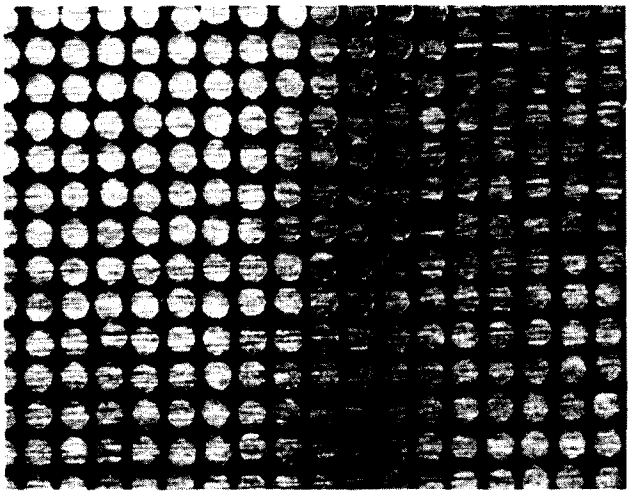

Fig. 5. Typical cross section of EPON-SST.

Matrix material

The matrix material used in the EPON-SST composite is an Epon 828 resin with a Z hardener. This material has been characterized by Sutherland and Lingle [8]. They found that the phase velocity C (mm/μsec) was dependent on the reduced angular frequency Ω† by

$$C = 2{\cdot}200 + (1{\cdot}796E\text{-}1)\log_{10}\Omega - (3{\cdot}911E\text{-}2)(\log_{10}\Omega)^2 + (7{\cdot}830E\text{-}3)(\log_{10}\Omega)^3 - (5{\cdot}754E\text{-}4)(\log_{10}\Omega)^4, 0 \leq \log_{10}\Omega \leq 7. \quad (14)$$

†The reduced frequency is the angular frequency ω multiplied by the time–temperature shift factor a_t, Eq. (8).

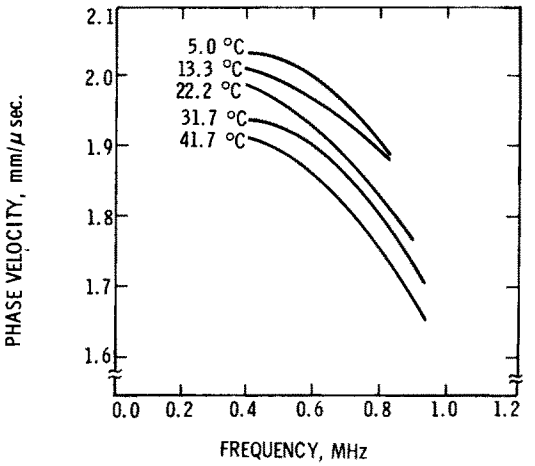

Fig. 6. Velocity dispersion spectra for EPON-SST at various temperatures.

This particular characterization is referenced to the glass transition temperature of 130°C and is based on an apparent activation energy (see Eq. (8)) of 8·9 kcal.

Using the data of Munson and May [9], Poisson's ratio at 25°C was determined to be 0·39 for this material.

This material is also described in the Appendix.

APPLICATION

Quartz phenolic

The application of the separation technique to the quartz phenolic data is accomplished by a close examination of the velocity spectra at various temperatures between the frequencies of 0·5 and 1·0 MHz (see Fig. 3). In this region, the slope is positive, which implies that the material is behaving in a viscoelastic manner. From this slope, one may deduce the apparent activation energy ΔH_a for the composite. Using the summary of data in Table 1, a plot of phase velocity vs temperature at 0·5 MHz was made along with the similar plot at 1·0 MHz shown in Fig. 2. From these two plots, ΔH_a may be determined from Eqs. (8) and (10). Namely, if

$$C(\omega_1)|_{T_1} = C(\omega_2)|_{T_2}, \tag{15}$$

then

$$\Delta H_a = R\frac{\log_{10}\omega_1 - \log_{10}\omega_2}{1/T_2 - 1/T_1}. \tag{16}$$

Using $\omega_1 = 0{\cdot}5$ MHz and $\omega_2 = 1{\cdot}0$ MHz, Eq. (16) was evaluated over the range of interest. The resulting average for ΔH_a was 36·3 kcal ($0°C \geq T \leq 40°C$).†

†Since ΔH_a is weakly dependent on the volume fractions of the constituents, it should be noted that the apparent activation energy computed here applies only to the composite considered. As discussed later, the viscoelastic characterization for the composite may be computed from homogeneous models for particular geometric arrays, but a similar analysis cannot be used with the 2D-QP data because the bulk properties of phenolic are not well known, and they do change when reinforcements are added.

Using an apparent activation energy of 36·3 kcal, a glass transition temperature T_g of 181°C[10], the 0·5 and 1·0 MHz temperature data, and Eqs. (8) and (10), the homogeneous phase velocity of the composite may be determined as a function of frequency for any temperature of interest. Doing this at 22·2°C, we obtain the viscoelastic characterization shown in Fig. 7. Also shown in Fig. 7 is the data obtained from the acoustic experiment at 22·2°C.

A similar comparison may be obtained for the exponential attenuation in the composite. As the data cited in Table 2 and Fig. 4 are all above the frequency region where geometric dispersion is small, a special series of tests were run at 1·0 MHz using the direct transmission technique cited by Sutherland[1]. The attenuation was found to be:

$$\alpha = 0{\cdot}01929 + 0{\cdot}00006912T \text{ (nepers/mm)}, 4°C \leq T \leq 45°C. \tag{17}$$

Using Eqs. (8), (11), (16) and (17), an apparent activation energy of 36·3 kcal, and a glass transition temperature of 181°C, the homogeneous attenuation of the composite may be determined. The results at 22·2°C are compared with the acoustic experiment in Fig. 8.

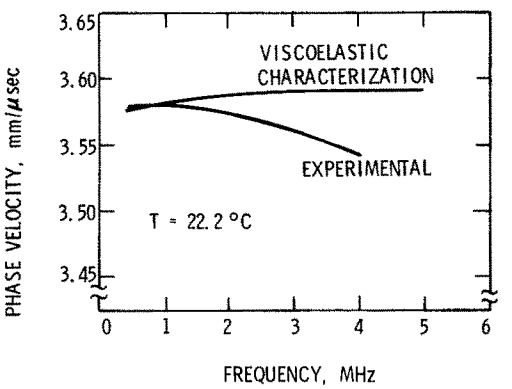

Fig. 7. Velocity dispersion spectra for quartz phenolic at 22·2°C.

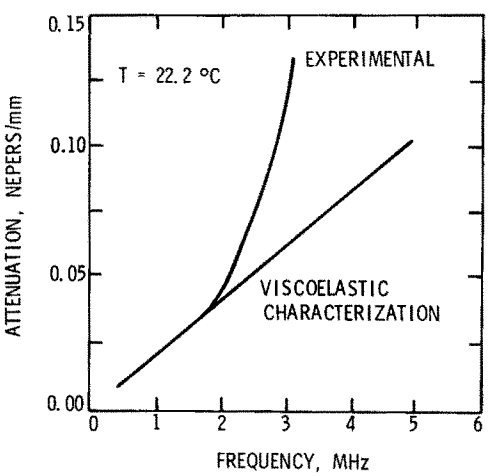

Fig. 8. Attenuation dispersion spectra for quartz phenolic at 22·2°C.

Figures 7 and 8 illustrate the relative importance of viscoelastic dispersion in this composite and display graphically the effects of its internal geometry on the propagation of waves through it. In Fig. 7, we see only a comparatively small decrease in velocity, which implies that the data are relatively far from the cutoff frequency of the first pass band (as previously surmised by Sutherland[1]) and that the internal geometry of this composite is not very important with respect to wave velocity. However, this is not the case for attenuation. In Fig. 8, we see a dramatic increase in the attenuation coefficient with the inclusion of internal geometry. As we are not close to the cutoff frequency, the attenuation produced by internal scattering is probably small and we conclude that some type of synergistic effect between viscoelastic and geometric dispersion is causing the large increase.

Now, rather than compare each spectrum separately, let us transform the acoustic data containing geometric dispersion according to Eqs. (8), (10) and (11) and compare the results with the viscoelastic characterization†. Doing this, we obtain the plot for velocity shown in Fig. 9 and for attenuation shown in Fig. 10. These plots, and Figs. 7 and 8 imply that for the temperature range investigated, the phase velocity of the composite is close to a homogeneous viscoelastic response, but the attenuation may differ markedly from the viscoelastic model.

EPON-SST

A close inspection of the velocity spectra obtained for the EPON-SST composite (see Fig. 6) indicates that for the frequency range investigated, this material is not behaving as a strictly viscoelastic material; i.e. nowhere do the spectra have a positive slope. Therefore, the method used to determine ΔH_a, and, thus the viscoelastic characterization, for the 2D-QP cannot be used here. However, since the Epon matrix is well characterized[8], we may deduce the homogeneous viscoelastic response of this material by using Hashin's model (i.e. by Eq. (13)), the viscoelastic

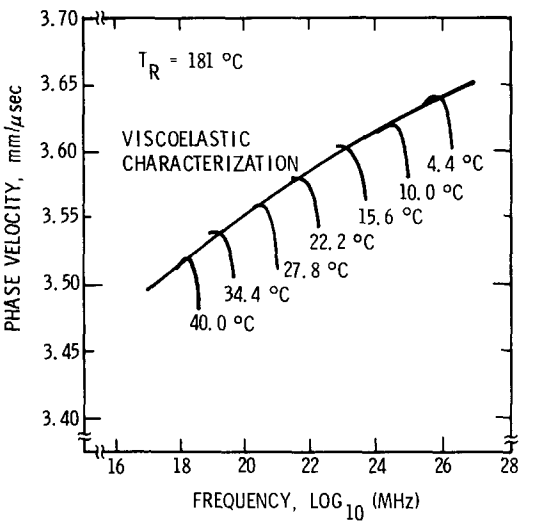

Fig. 9. Summary of velocity dispersion spectra for quartz phenolic.

†This transformation is only valid for comparison purposes, because time–temperature superposition only holds for linear viscoelastic materials. However, ambiguities in the abscissa may be easily rectified by referencing the scale to the temperature of interest.

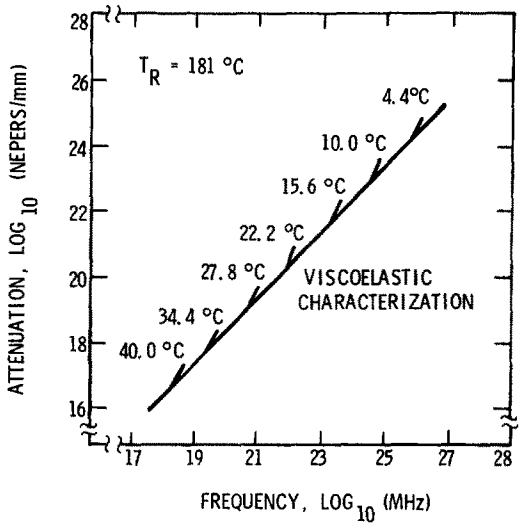

Fig. 10. Summary of attenuation dispersion spectra for quartz phenolic.

characterization of the Epon matrix, Eq. (14), and by assuming a time-independent Poisson's ratio of 0·39[9]. The lower bound on phase velocity, as a function of the reduced frequency Ω, becomes

$$C(\Omega) = 0{\cdot}788 C_m(\Omega), \quad 0 \leq \log_{10}(\Omega) \leq 7, \tag{18}$$

where $C_m(\Omega)$ is given by Eq. (14).

Transforming Eq. (18) to 22·2°C by using Eq. (8) with an apparent activation energy of 8·9 kcal, the homogeneous viscoelastic characterization (Hashin's lower bound) for this temperature, shown in Fig. 11, is obtained. Along with the viscoelastic characterization, the dispersion spectrum for the composite obtained at 22·2°C is plotted.

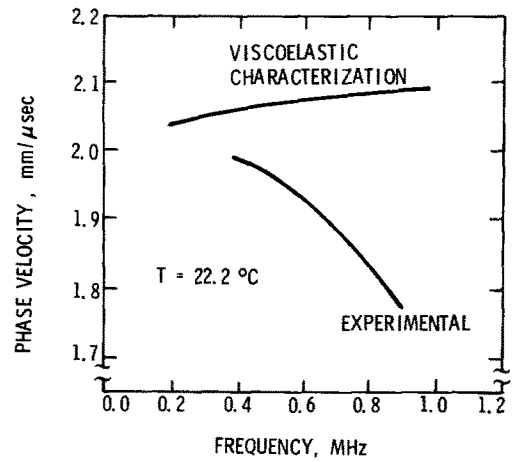

Fig. 11. Velocity dispersion spectra for EPON-SST at 22·2°C.

Figure 11 illustrates that viscoelastic dispersion plays a minor role in the total dispersion spectrum of this composite. In contrast to the 2D-QP data displayed in Fig. 7, we note that as the frequency increases, there is a marked divergence of the composite's velocity spectrum from the viscoelastic spectrum. This divergence indicates that the data are relatively close to the cutoff frequency of the first pass band. Further, the importance of geometric dispersion is illustrated in the low frequency data of the spectrum. As the two spectra do not intercept at the low frequency data of the spectrum. As the two spectra do not intercept at the low frequency end, geometric dispersion must still be important in this composite, even at 0·4 MHz. And, indeed, an extrapolation of the composite's spectrum would indicate that geometric dispersion is important down to 0·2 MHz.

Again, to compare the acoustic data to the viscoelastic characterization, let us transform the data according to Eqs. (8), (10) and (11) with ΔH_a equal to 8·9 kcal. The comparison is shown in Fig. 12. These plots imply that for the temperature and frequency ranges investigated, the homogeneous viscoelastic characterization of this material is not an adequate representation of the composite's behavior.

CONCLUDING REMARKS

Two methods to separate viscoelastic dispersion from the total dispersion spectrum of a fiber reinforced viscoelastic material have been presented here. The first method constructs a homogeneous viscoelastic model of the composite from the low-frequency dispersion spectrum of the composite at several temperatures. The advantages of this method are that very little must be known about the properties of the constituents and the method is not restricted to any specific internal geometries. Its main disadvantages are that it requires spectra at several temperatures and it is restricted to composite materials whose internal geometries have a characteristic dimension sufficiently small to allow acoustic experiments in a range where geometric dispersion is small. The second method constructs a homogeneous model from the properties of the composite's constituents. The obvious disadvantages are that each constituent must be well characterized and a homogeneous model must be constructed for the composite's particular

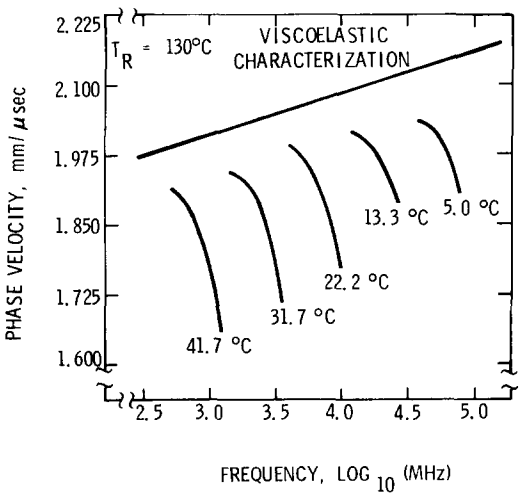

Fig. 12. Summary of velocity dispersion spectra for EPON-SST.

internal geometry, but its advantage is that the spectrum of composite need be determined only at the temperature and frequency range of interest.

APPENDIX—MATERIAL DESCRIPTION

Cloth-laminate quartz phenolic

The first material studied in this investigation, a cloth-laminate quartz phenolic (2D-QP), was fabricated from Astroquartz 503 (Bendix Corporation; Kansas City) and Evercoat 201 phenolic resin (Evercoat Chemical Co.; Santa Fe Springs, California). The quartz cloth was cut to the desired size, impregnated with phenolic, and stacked in a mold. The composite-mold assembly was then placed in an oven preheated to 94°C. When the composite's temperature reached 82°C, the assembly was removed from the oven and placed in a press with platens preheated to 121°C. When the temperature of the composite reached 94°C, a pressure of 34·4 Mdynes/cm^2 was applied; at 102°C, the pressure was increased to 97·4 Mdynes/cm^2; at 116°C, the platen temperature was increased to 163°C; and, at 163°C, the pressure and temperature were held for 8 hr. The composite sample produced for this study was 30·5 cm square by 5·08 cm thick with 540 plies. The bulk density was 1·832 gm/cm^3.

This particular fabrication technique was chosen because it produced consistent material properties and the composite was relatively free of voids. To ensure maximum reproducibility between the samples, several were machined from the center section of the bulk composite. Those samples which had the closest match of density and ultrasonic wave velocity at 1 MHz and 22·2°C were chosen for the study. Upon completion of the ultrasonic experiments, each sample was destroyed in a quantiative ash experiment, in order to determine the weight fraction of quartz. Using the weight fraction of quartz, the bulk densities of silica (quartz), 2·20 gm/cm^3, and phenolic, 1·26 gm/cm^3, a theoretical density was calculated and the percent void content was determined. The percent void content was found to vary from 1·4 percent to 1·7 percent in the three samples[1].

Epon–stainless steel

The second material studied, stainless steel reinforced epoxy, was fabricated by Haveg Industries, Inc. (Reinhold Aerospace Division; Santa Fe Springs, California) from 0·457 mm dia, 304-stainless steel wires and Epon 828 resin (Shell Chemical Corporation) with Z hardener. The SST wires were drawn, cut, straightened, and individually placed in a layup fixture at approximately 250 fibers/cm^2 in a square array. After an inspection for misalignment, the layup was rinsed with methyl ethyl ketone (MEK), acid etched for 10 min in concentrated hydrochloric acid at ambient temperature, rinsed in flowing water for 5 min, rinsed in distilled water and air dried, rinsed in MEK, and oven dried and preheated 30 min at 66°C. The resin batch was then mixed and evacuated. The layup was removed from the oven and placed in a casting mold. After the resin batch was added and degassed, the resin was cured and then postcured at 122°C. Samples were cut from the billet.

The specimens obtained in this manner had a 40·7 theoretical volume percentage of stainless steel, 7·90 gm/cm^3, and the bulk density of Epon 828-Z, 1·202 gm/cm^3, the predicted density of the composite is 3·93 gm/cm^3. This value compares well with a measured density of 3·85 gm/cm^3[1].

Epon 828-Z

The Epon 828 epoxy (produced by Shell Chemical Corporation) is a condensation product of epichlorohydrin and bisphenol-A, with no dilutents. Epoxide equivalents are controlled to give 183–195 gram of resin per gram atom of epoxy group. This polymer has physical and mechanical

properties which depend upon the hardening agent and processing details. Hardener Z is an aromatic eutectic mixture of methylene dianaline, MPDA (metaphenylenediamine), and phenyl glycidyl ether. Curing procedure for this hardener was 4 hr at room temperature followed by 4 hr at 55°C and 16 hr at 93°C. The properties for this cure are very similar to those of the matrix used in the EPON-SST composite. The glass transition temperature is 130°C and its density is 1·202 gm/cm^3 [8, 9].

REFERENCES

1. H. J. Sutherland, Dispersion of Acoustic Waves by Fiber-Reinforced Viscoelastic Materials. 86*th Meet.*, *Acoustical Society of America*, Los Angeles, October 30 to November 2 (1973).
2. J. W. Nunziato and H. J. Sutherland, Acoustical Determination of Stress Relaxation Functions for Polymers, *J. appl. Phys.* **44**, 184 (1973).
3. B. D. Coleman and W. Noll, Foundations of Linear Viscoelasticity. *Rev. Mod. Phys.* **33**, 239 (1961); Erratum *Ibid.* **36**, 1103 (1964).
4. S. C. Hunter, Viscoelastic Waves, *Progress in Solid Mechanics*, Vol. 1, edited by I. N. Sneddon and R. Hill. North-Holland Publishing Co. (1960).
5. Z. Hashin, Viscoelastic Fiber Reinforced Materials. *AIAA J.* **4**, 1411 (1966).
6. H. J. Sutherland and H. H. Calvit, A Dynamic Investigation of Fiber-Reinforced Viscoelastic Materials. *Experimental Mechanics* **14**, 304 (1974).
7. J. D. Ferry, *Viscoelastic Properties of Polymers*. Wiley (1961).
8. H. J. Sutherland and R. Lingle, An Acoustic Characterization of Polymethyl Methacrylate and Three Epoxy Formulations *J. appl. Phys.* **43**, 4022 (1972).
9. D. E. Munson and R. P. May, Dynamically Determined High-Pressure Compressibilities of Three Epoxy Resin Systems *J. appl. Phys.* **43**, 962 (1972).
10. M. F. Furney, Sandia Laboratories, Private communication.